Beni-Suef University Journal of Basic and Applied Sciences

RESEARCH

Open Access

# Comparative study of the reptilian cornea's microstructure

Zeinab Abdelftah[1], Ahmed Ragab[1], Rasha E. Abo-Eleneen[1], Abdelaziz S. Abuelsaad[1] and Ahlam M. EL-Bakry[1*]

## Abstract

**Background** The cornea of various vertebrate is considered a major part in the glop, which acts as a powerful lens, providing a sharp retinal image, and meantime acts as an excellent defensor for other corneal layers.

**Results** The four reptilian families [Scincidae (*Chalcides ocellatus*); Chamaeleontidae (*Chameleon chameleon*); Cheloniidae (*Chelonia mydas*) and Testudiniae (*Testudo kleinmanni*)] investigated in the current study were gathered across Egypt. After being taken out of the orbit, the cornea under inquiry was ready for light, specific stain and scanning electron microscopy. The epithelium, stroma, and endothelium are the three corneal layers that are common to all four species of reptiles. All other species lack Bowmen's and Descemet's membranes, with the exception of *C. ocellatus* and *T. kleinmanni*. The latter layers of *Chalcides ocellatus* display a strong affinity for Periodic Acid Schiff stain. Epithelial cells with a variety of forms, from hexagonal to atypical polygonal cells, cover the outer corneal surface. These epithelial cells are coated in short microplicae, microvilli, and microholes of varied diameters. There are a few blebs scattered around their surface.

**Conclusion** The current study concluded that various habitats have various significant effects on the cornea's microstructure characteristics and its physiological trends to accommodate different environmental surroundings.

**Keywords** Reptiles, Cornea, Stroma, Blebs, Microprojections, Microplicae, Microvilli

## 1 Background

Our eyes make sense of our lives, as they reflect everything beautiful around us to our soul. Eyes are an important biologic organ in most vertebrate animals as the morphological character and physiological function of the eye reflect the organism's life system and its habitation [1, 2]. The transparency of vertebral cornea has a vital effect on clear vision. The cornea acts as a permeable surface that refracts and transmits the light to the lens and the retina [3]. In the eyes of humans and other terrestrial vertebrates, the cornea serves as the outermost refractive surface. The entire refractive power of the eye is about 70%. It accounts for roughly 70% of the eye's overall refractive power [4]. In some reptilian species, the refractive power of cornea represents the total power to compensate for the absence of refractive power of the lens [5].

The corneal composition of various mammals and animal species has drawn attention and was the focus of many studies [6–9]. On the other hand, little investigations have been conducted on many vertebrates like amphibians, reptiles and aves [5, 10–12]. The cornea is considered a peculiar modification of a variety of connective tissue. Reptile eyes resembled mammals; their lens are pushed further forward to form a sharp retinal image. The cornea of most tetrapod is composed of three structural layers, including a stratified epithelial layer with protective and sensory function, hypocellular stroma of collagenous materials, and a regulator of corneal hydration endothelial layer [13, 14].

*Correspondence:
Ahlam M. EL-Bakry
amalbakry2@yahoo.com
[1] Zoology Department, Faculty of Science, Beni-Suef University, Beni-Suef 62511, Egypt

In several vertebrates, the corneal layers' main energy source is provided by polysaccharides. Corneal epithelium represents large stores of polysaccharides in various vertebrates [15]. A refracting cornea is covered with many cell regulator microprojections, such as microridges, microplicae, microvilli, microholes and cilia, that aid in the physiological function of the cornea. About the corneal surface, each of the cell surface regularities has a pivotal function for ensuring the formation of a sharp retinal image. Besides maintaining a stable structure for the corneal epithelial and healthy environment, the microprojections cover the epithelial surface [5, 8]. Scanning electron microscope revealed many microprojections covering the corneal surface of salamander *Triturus* Cristatus [16, 17] and cornea of veiled chameleon (*Chamaeleo caly ptratus*) [5].

Generally, the morphological and histological structure of Reptilian's vital organs is varied because of their adaptation to environmental conditions. Consequently, cornea is reported by many authors [18–21]. Probably due to insufficient sensitivity of some investigations, recent data are somewhat contradictory, and others are either describing or denying the existence of the microstructures in different species of turtles, lizards and snakes [22].

To the best of our knowledge, based on reviewing related literature, no electron-microscopic clarifications of the reptilian corneal' layers have been published up to now. As a result, the current study's objective was to examine the histological, histochemical and scanning electron architectures and to correlate them with the alterations in the habitat of some reptilian species.

Additionally, the study also shows a relationship between the morphological and anatomical characteristics of the cornea for a number of species of reptiles and the major impact of the environmental state.

## 2 Methods

### 2.1 Experimental animals

Four reptilian families [Scincidae (*Chalcides ocellatus*), Chamaeleontidae (*Chameleon chameleon*), Cheloniidae (*Chelonia mydas*) and Testudiniae (*Testudo kleinmanni*)] were gathered from several Egypt places. They were identified recently by El Din [23]. Ten adult animals from each species were investigated, with weight ranged from 70.0 ± 2.4 g in *C. ocellatus*, 140.0 ± 10.0 g in *C. chameleon*, 770.0 ± 34.6 g in *C. mydas* and 900.0 ± 30.7 g in *T. kleinmanni*. The current study provided the following information about their common name, distribution in Egypt, and habitat as follows:

#### *2.1.1 Family scincidae*

*Chalcides ocellatus* (Forsskål, 1775). The common name is Eyed Skink and Ocellated Skin. They distributed in the Eastern desert of Egypt (25.1077°N–33.7965°E) and Abu - Rawash (30.0131°N–31.2089°E). According to Leviton, Anderson [24], it inhabited sandy desert and banks of irrigation canals in the Nile Valley and Delta and they had diurnal activity.

#### *2.1.2 Family chamaeleontidae*

*Chameleon chameleon* (Rafinesque, 1815). The common name is Herbaya. They distributed in Abu- Rawash (30.0131°N–31.2089°E) and rainy area as Behaira (30.8481°N–30.3436° E). It lived in desert regions with vegetation and trees, and it would descend to the ground to migrate from one bush to another. They inhabited all kinds of tropical and mountain rain forests, and sometimes deserts and steppes, and activated during the day [25, 26].

#### *2.1.3 Family cheloniidae*

*Chelonia mydas* (Linnaeus, 1758): the common name is a Green sea turtle. The main distribution area in Egypt was recorded as Red sea coasts (20.2802°N, 38.5126°E). With two different populations in the Atlantic and Pacific oceans, as well as the Indian Ocean, it was distributed throughout the world's tropical and subtropical seas. In addition to their primarily daily activity, they engaged in nocturnal activities [27].

#### *2.1.4 Family testudiniae (Testudo kleinmanni; Lortet, 1883)*

The common name is African spurred tortoise or Egyptian tortoise. They distributed in the Eastern desert of Egypt (25.1077°N, 33.7965°E) and Abu-Rawash (30.0131°N, 31.2089°E). They were diurnal reptilian; that inhabit semiarid and arid environments with compact sand and gravel plains, strewn boulders, and salt marshes along the coast [28]. It is primarily found in dry to semiarid coastal dunes and shallow sandy/rocky valleys along the Mediterranean coast up to around 90–120 km of Egypt, from western Libya to the eastern–north Sinai Peninsula [29, 30]. The smallest desert-dwelling Testudine found in the areas surrounding the Mediterranean and the Middle East is the Egyptian tortoise (*Testudo kleinmanni Lortet,* 1883) [31]. Its small size and vividly colored carapace offer effective camouflage [32].

### 2.2 Experimental methods

The corneas were prepared for histological, histochemical, and scanning electron examination by cutting

them loose from the orbit following enucleation with a sharpened razor blade.

#### *2.2.1 Histological sections*

To get rid of the extra fixative that had been employed, the fixed corneal specimens were washed. After that, they were dehydrated for 45 min in ethyl alcohol of varying concentrations (70, 80, 90, and 95%) before spending another 30 min in each of two changes of 100% ethyl alcohol. After that, cleaning in two changes of xylene took place for a total of 30 min. After being impregnated with paraplast plus (three changes) for three hours at 60 °C, the tissues were then implanted in paraplast plus. Slices with a thickness of 4–5 mm were stained with hematoxylin and eosin for histological analysis [33]. The presence or absence of several layers was noted after analysis of the corneal histological sections, and the results were as follows: absent (−); one layer (+); two layers (++); and three layers (+++).

#### *2.2.2 Histochemical sections (periodic acid-Schiff's) [34]*

The fixed specimens were rehydrated using graded ethanol to water after being de-waxicated by xylene. Then, for five minutes, they were exposed to an oxidation process using aqueous periodic acid solution 1% (H5IO6—WINLAB; Leicestershire, UK). After being covered with Schiff's reagent for 10 to 15 min, they were rinsed with distilled water before being rinsed for five minutes under running water. The specimens were then mounted on slips, dehydrated, and made clear with xylene. The slices were prepared for examination with light microscopy [35, 36]. The amount of carbohydrates was assessed and denoted by the following symbols: − is absent; + is mild; ++ is moderate, +++ is high.

#### *2.2.3 Scanning electron microscopy (SEM)*

According to Morris [37], a modified Karnovsky solution (2% paraformaldehyde and 2.5% glutaraldehyde with 0.1 M cacodylate-buffer, pH 7.4) was used to fix the whole eye overnight. Then, the fixed specimens were post-fixed for two hours at 37 °C in a cacodylate-buffered solution containing 1% osmium tetroxide after being washed in 0.1 M cacodylate buffer. To begin the dehydration process, the corneal specimens were washed in ethanol at increasing concentrations. The initial rinse took place in 50% ethanol for 5 min, was followed by 3 rinses in 70% ethanol for 5 min, 3 rinses in 90% ethanol for 5 min, 2 rinses in 100% ethanol for 5 min, and finally 2 rinses in 100% ethanol for 10 min (molecular sieve). Hexa-methyldisilane (HMDS) was substituted for all of the ethanol in the samples, and the fume hood was left in place for 10 min. The tops of the metal SEM stubs, which were similarly labeled, were covered with double-sided carbon tape. Joel's fine coat Ion Sputter (SPI-Module) was then used to sputter gold onto the dried samples. At the Microanalysis Center, Beni-Suef University, Faculty of Science, Egypt, specimens were examined and recorded on camera using industry-standard microscope operating procedures. The examination was started at a low magnification and increased at a 15-kv accelerating voltage (JSM.5400LV, JEOL) [38, 39].

#### *2.2.4 Image analysis*

JEOL (JSM with accelerating voltage 5400 LV) was used to examine the anterior surface of the cornea in each of the studied species. Number of cells and area ($\mu m^2$) of each individual epithelial cell were measured [40]. In addition, the mean epithelial cell density, the diameters of microholes and blebs were calculated. By using Image J software, these image analyses were digitally recorded.

### 2.3 Statistical analysis

One-way analysis of variance (ANOVA) was used to analyze the data. Mean for at least 10 measurements of each characteristic (microholes and blebs) on the corneal surface. Mean ± Standard deviation (SD) were used to represent the data. *P* values that were greater than 0.05 ($P > 0.05$) were regarded statistically as non-significant, whereas *P* values that were less than 0.05 ($P < 0.05$) were considered statistically significant.

### 2.4 Ethics Committee approval

All animal procedures were carried out in compliance with the standards established in the guidelines for the care and use of experimental animals by the Animal Ethics Committee of the Zoology Department in the Faculty of Science at Beni-Suef University (under approval number BSU/FS/2015/9).

## 3 Results

### 3.1 Histological observations

Both Fig. 1a, b and Table 1 illustrate different sections of the cornea in (*C. ocellatus*), which consists of the simple epithelium. It is formed of one layer of cuboidal cells. Besides, the endothelium is represented by a single layer of flat squamous cells. Data recorded the presence of both Bowman's and Descemet's membrane. Additionally, *C. ocellatus*' corneal sections have a stromal matrix with very few keratocytes Moreover, the corneal sections of *C. ocellatus* have a stromal matrix.

The histological structure of corneal sections of *C. chameleon* revealed the presence of two cellular layers, epithelium and endothelium, and the stromal layer. The outer layer epithelium is composed of an inner layer of basal cuboidal cells with round nucleus covered by another layer of flat squamous cells. The endothelium

appears as a monolayer of flat squamous cells. Keratocytes are evenly distributed throughout the stromal matrix, and the collagen fibrils of the stroma can be divided into two primary zones: the outer lamellar zone, which has loose fibrils, and the inner lamellar zone, which has condensed fibrils (Fig. 2a, b, Table 2).

Similarly, the corneal histological sections of *Chelonia mydas* represent the ideal structure of cornea (Fig. 3a, b and Table 1). The epithelium is made up of two layers of polyhedral cells, an outer layer of flat squamous cells, and an inner layer of basal columnar cells. Besides, the stromal matrix has a good distribution of keratocytes.. Squamous flat cells make up the endothelium layer, which separates the cornea from other optical components. Additionally, it was noted that *Chelonia mydas* and *C. chameleon* lacked both Bowman's membrane and Descemet's membrane.

*Testudo kleinmanni* corneal sections are shown in Fig. 4a, b and Table 1. They are made of an outer epithelium represented by one layer of basal short columnar cells, three superficial layers of polyhedral cells, and a final layer of flat squamous cells. Both Bowman's and Descemet's membranes are located at the base of the epithelium and endothelium, the two cellular layers. In addition, the stroma is packed with uniformly distributed collagen lamellae and keratocytes. However, the

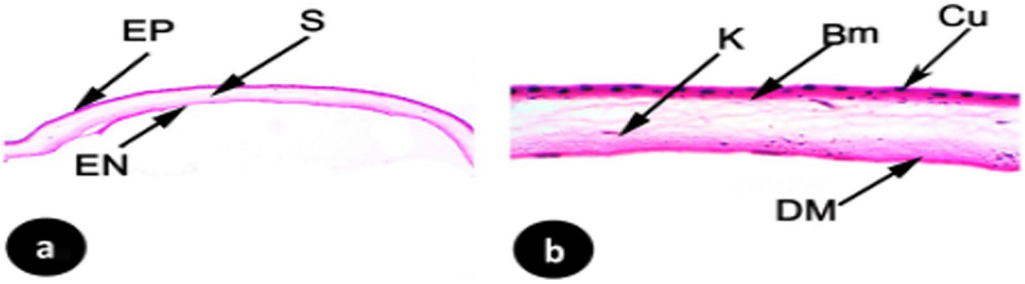


**Fig. 1** Photomicrographs of corneal transverse section of *Chalcides ocellatus* showing **a** epithelium (EP), stroma (S) and endothelium (EN), (H&E X 100). **b** Higher magnification of **a**, showing keratocytes (K), Bowman's membrane (B), Descemet's membrane and cuboidal cells (Cu) (H&E X400)

**Table 1** Comparison of the histological structure of the corneal epithelium in four species of reptiles

| Species | Types of epithelial's cells | | | | Bowman's membrane | Stroma membrane | | Descemet's membrane | Endothelium |
|---|---|---|---|---|---|---|---|---|---|
| | Basal columnar | Basal cuboidal | Polyhedral | Flat squamous | | | | | |
| *Chalcides ocellatus* | – | + | – | – | + | + | | + | + |
| *Chameleon* | – | + | – | + | – | OLZ+ | ILZ+ | – | + |
| *Chelonia mydas* | + | – | ++ | + | – | + | | – | + |
| *Testudo kleinmanni* | + | – | +++ | + | + | + | | + | + |

Absence (–), one layer (+), two layers (++), and three layers (+++); *OLZ* outer lamellar zone; *ILZ* inner lamellar zone

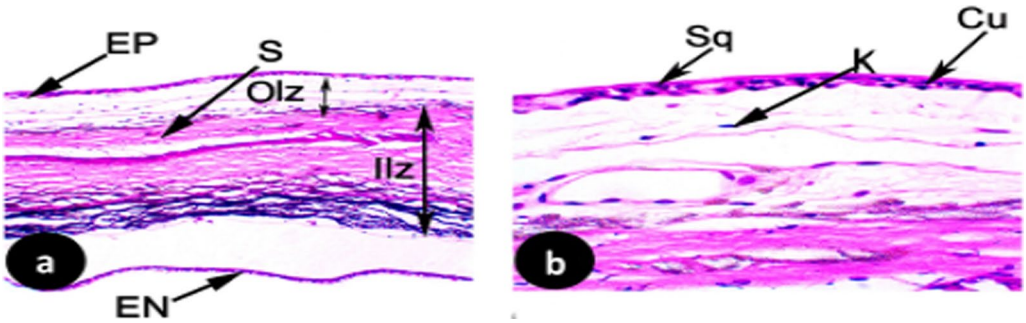


**Fig. 2** Photomicrographs of corneal transverse section of *Chameleon*, showing **a** epithelium (EP), stroma (S), stroma's outer lamellar zone (OLZ), stroma's inner lamellar zone (ILZ) and endothelium (EN) (H&E X 100). **b** Higher magnification of **a**, showing squamous cells (Sq), cuboidal cells (Cu) and keratocytes (K) (H&E X 400)

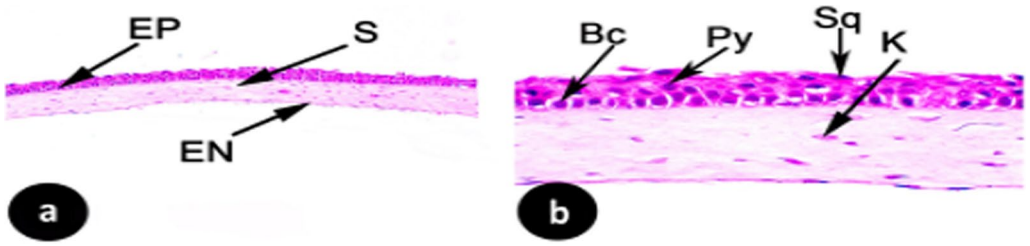


**Fig. 3** Photomicrographs of corneal transverse section of *Chelonia mydas*, showing **a** epithelium (EP), stroma (S) and endothelium (EN) (H&E X 100). **b** Higher magnification of **a**, showing squamous cells (Sq), polyhedral cells (Py), basal columnar cells (Bc) and keratocytes (K) (H& E X 400)

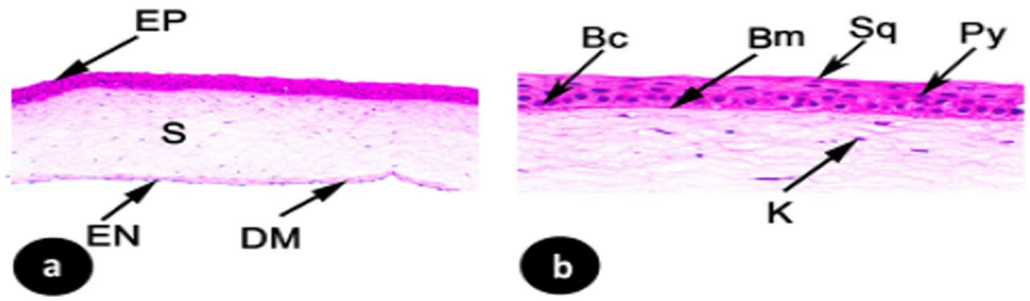


**Fig. 4** Photomicrographs of corneal transverse section of *Testudo kleinmanni*, showing epithelium (EP), stroma (S), Descemet's membrane and endothelium (EN) (H&E X100). **b** Higher magnification of **a**, showing keratocytes (K), squamous cell (Sq), polyhedral cell (Py), basal columnar cell (Bc) and Bowman's membrane (B) (H& E X400)

**Table 2** Comparison of the corneal layer thicknesses (mean ± SD) in four reptilian's species (10 animals per species)

| Species | Total cornea thickness (μm) | Corneal layers | | |
|---|---|---|---|---|
| | | Epithelium thickness (μm) (%) | Stroma thickness (μm) (%) | Endothelium thickness (μm) (%) |
| *Chalcides ocellatus* | $45.8 \pm 9.7^{a}$ | $7.4 \pm 0.7^{b}$ (16.1%) | $36.3 \pm 9.2^{a}$ (79.2%) | $2.7 \pm 0.2^{b}$ (5.8%) |
| *Chameleon* | $112.8 \pm 8.3^{c}$ | $3.7 \pm 0.3^{a}$ (3.2%) | $106.8 \pm 13.4^{c}$ (94.6%) | $2.3 \pm 0.1^{b}$ (2%) |
| *Chelonia mydas* | $80.1 \pm 7.7^{b}$ | $28.8 \pm 3.5^{c}$ (35.9%) | $50.7 \pm 9.8^{b}$ (63.2%) | $2.0 \pm 0.01^{a}$ (2%) |
| *Testudo kleinmanni* | $202.7 \pm 18.7^{d}$ | $32.4 \pm 4.4^{d}$ (15.9%) | $166.8 \pm 16.1^{d}$ (82.2%) | $3.4 \pm 0.6^{c}$ (1.6%) |
| *F* value | 578.4 | 1152.7 | 563.0 | 38.6 |
| *P* value | 0.000 | 0.001 | 0.001 | 0.001 |

Layer's thickness that not sharing common superscripts denotes significant differences ($P < 0.05$)

endothelium is represented by a single layer of flat squamous cells. Significant variance ($P < 0.001$) is shown in Table 2 for the total cornea thickness between the different species with an average of 45.80 ± 9.70, 112.80 ± 8.30, 80.10 ± 7.70 and 202.7 ± 18.70 μm for *C. ocellatus, C. chameleon, C. mydas* and *T. kleinmanni*, respectively. Moreover, there are variations in the epithelial layers thickness with an average value of 7.4 ± 0.7, 3.7 ± 0.7, 28.8 ± 3.5 and 32.4 ± 4.4 μm that represented 16.1, 2.9, 35.9, and 15.9% of total corneal thickness for *C. ocellatus, C. chameleon, C. mydas* and *T. kleinmanni*, respectively. As a result, Table 2 shows that there is a significant relationship between all examined reptile species ($P > 0.001$).

Regarding stromal thickness, it was noted that there is a significant relationship between corneal stromal thickness of *C. ocellatus*, *C. chameleon*, *C. mydas* and *T. kleinmanni* and recorded 36.3 ± 9.2 (79.2%), 106.8 ± 13.4 (94.6%), 50.7 ± 9.8 (63.2%) and 166.8 ± 16.1

(82.2%), respectively (Table 2). However, endothelium layer showed significant variation ($P > 0.001$), whereas *C. ocellatus, C. chameleon, C. mydas* and *T. kleinmanni* recorded thickness as 2.7 ± 0.2 µm (5.8%), 2.3 ± 0.1 µm (2%), 2.0 ± 0.01 µm (2%) and 3.4 ± 0.6 µm (1.6%), respectively (Table 2).

To summarize the present data, Table 2 reveals that, among the investigated reptilian cornea's epithelia, *C. mydas* has the thickest epithelial layer (35.9%), whereas the thickest stroma layer was recorded for *C. chameleon* (94.6%). Moreover, *C. ocellatus* has the thickest endothelium layer (5.8%) incomparable to other reptilian cornea's endothelial.

**Table 3** Comparison of the amounts of carbohydrates found in the corneas of the four examined reptile species by using (periodic acid-Schiff (PAS) stain): symbols refer to (+++) strong reaction; (++) moderate reaction; (+) weak reaction; (–) absent

| Corneal layers | | | | | | |
|---|---|---|---|---|---|---|
| **Species** | **Epithelium** | **Bowman's membrane** | **Stroma** | | **Descemet's membrane** | **Endothelium** |
| *Chalcides ocellatus* | ++ | +++ | + | +++ | +++ | |
| *Chameleon* | ++ | – | +(OLZ) | ++(ILZ) | – | ++ |
| *Chelonia mydas* | ++ | – | +++ | – | +++ | |
| *Testudo kleinmanni* | +++ | – | ++ | – | +++ | |

*OLZ* outer lamellar zone, *ILZ* inner lamellar zone

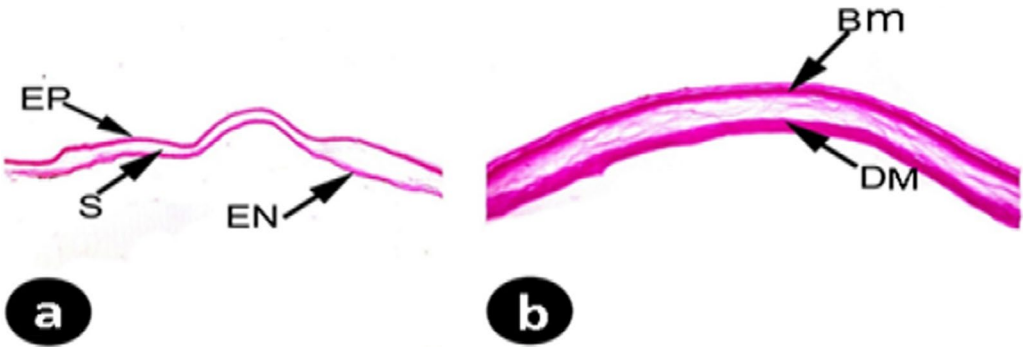


**Fig. 5** A light micrograph of *Chalcides ocellatus'* transverse corneal section, showing **a** epithelium (EP) had moderate content of polysaccharides, endothelium (EN) had a high content of polysaccharides and stroma (S) appear weakly stained (PAS X100). **b** Higher magnification of **a**, showing high PAS activity in Bowman's membrane (B) and Descemet's membrane (PAS X400)

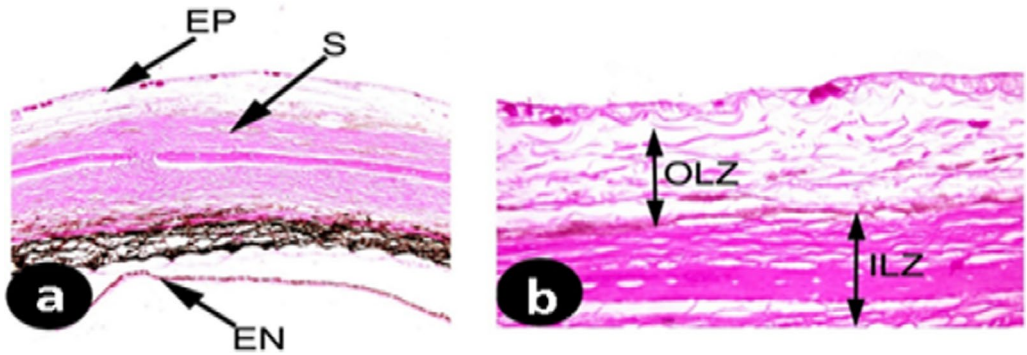


**Fig. 6** A light micrograph of *Chameleon '* transverse corneal section, showing **a**: moderate amount of PAS-positive materials in the stroma (S), endothelium (EN) and epithelium (EP) (PAS X100). **b** Higher magnification of **a**, displaying outer lamellar zone (OLZ) of the stroma had very low activity of PAS reaction and inner lamellar zone (ILZ) had moderate content of polysaccharides (PAS X400)

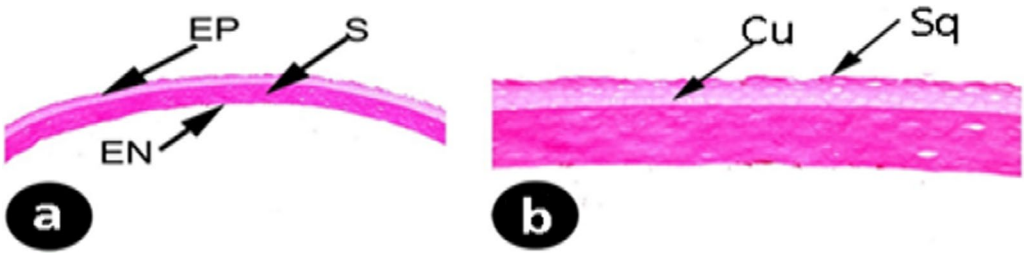


**Fig. 7** A light micrograph of *Chelonia mydas* transverse corneal section, exhibiting **a**: moderate PAS-positive reaction in the epithelium (EP). Stroma (S) and endothelium (EN) appear strongly stained (PAS X100). **b** Higher magnification of **a**, displaying high activity of PAS reaction at squamous epithelial cells (Sq). Basal cuboidal epithelial cells (Cu) appear low PAS-positive reaction. (PAS X400)

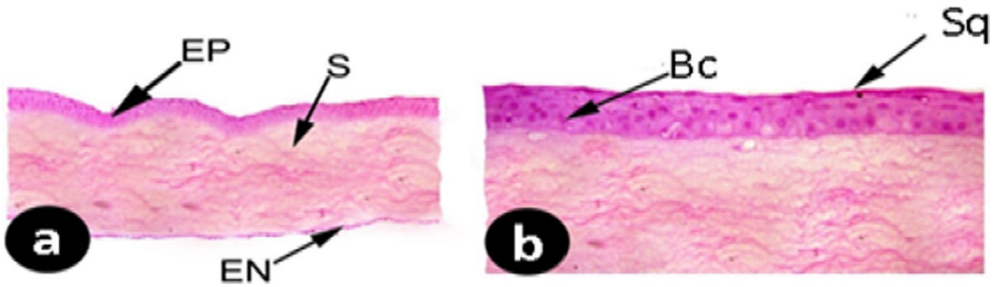


**Fig. 8** A light micrograph of *Testudo kleinmanni* transverse corneal section, exhibiting **a** high PAS-positive materials in the epithelium (EP) and endothelium (EN). Stroma (S) was moderately stained (PAS X100). **b** Higher magnification of Fig. [41], displaying high activity of PAS reaction at squamous epithelial cells (Sq). Basal columnar epithelial cells (BC) appear moderate PAS-positive reaction (PASX400)

### 3.2 Histochemical observations

Table 3 and Figs. 5a, b, 6a, b, 7a, b and 8a, b reveal that *T. kleinmanni* has a highly positive PAS reaction in the corneal epithelial layer, whereas *C. ocellatus, C. chameleon and C. mydas* exhibit a moderate PAS reaction (Figs. 5a, 6a, 7a, 8a). Furthermore, there was strong PAS-positive reaction in the stroma of *C. mydas* and was moderately stained in the inner lamellar zone of *C. chameleon* and *T. kleinmanni*. However, it appeared weakly stained in *C. ocellatus* and the outer lamellar zone of *C. chameleon*. Moreover, Bowman's membrane and Descemet's membrane showed strong PAS-positive reaction only in *C. ocellatus* (Fig. 5b). It was obvious that heavy stain was recorded in the endothelium of *C. ocellatus*, *C. mydas* and *T. Kleinmanni*, whereas moderate stained affinity was recorded in *C. chameleon*.

### 3.3 SEM observations

The cell densities of reptilian species show high significance ($P<0.000$), which varied between 4985.20 ± 200.0 cells/mm2 for *C. chameleon*, 4515.7 ± 254.3 cells/mm$^2$ in *C. ocellatus*, 3682.66 ± 162.5 cells/mm$^2$ in *Testudo kleinmanni*, however, and 3675.9 ± 327.4 cells/mm$^2$ in *C. mydas* (Table 4).

In addition, the central cornea of four investigated reptilian species possesses different types of epithelial cells, which vary from the hexagonal shape in *C. ocellatus* (Fig. 9a) to regular polygonal in *C. mydas* (Fig. 9c) and irregular polygonal cells in *C. chameleon* and *Testudo kleinmanni* (Fig. 9b, d, respectively).

Depressions (De) appear at the central corneal surface and are considered as the main character in the cornea of three studied reptilian species (*C. chameleon, C. mydas* and *T. kleinmanni*), which represented small breaks at the cell membrane. Microplicae are composed of a complex of tiny projections that overlap and are distributed over the corneal surface. They are sorted into three types

**Table 4** Comparison of the cell density (Mean ± SD) and diameter of blebs and microholes in corneal epithelial layer of four reptilians species (10 animals per species)

| *Species* | Epithelial cell density (cells/mm$^2$) | Blebs (μm) | Microholes (μm) |
|---|---|---|---|
| *Chalcides Ocellatus* | 4515.7 ± 254.3$^b$ | NM | 4.9 ± 0.7$^c$ |
| *Chameleon* | 4985.2 ± 200.0$^c$ | NM | 0.8 ± 0.1$^b$ |
| *Chelonia mydas* | 3675.9 ± 327.4$^a$ | NM | 1.0 ± 0.2$^b$ |
| *Testudo kleinmanni* | 3682.6 ± 162.5$^a$ | 0.90 ± 0.05 | 0.3 ± 0.02$^a$ |
| *F* value | 42.2 | NM | 188 |
| *P* value | 0.000 | NM | 0.000 |

Measurements that not sharing common superscripts denote significant differences ($P<0.05$). *NM* not measured

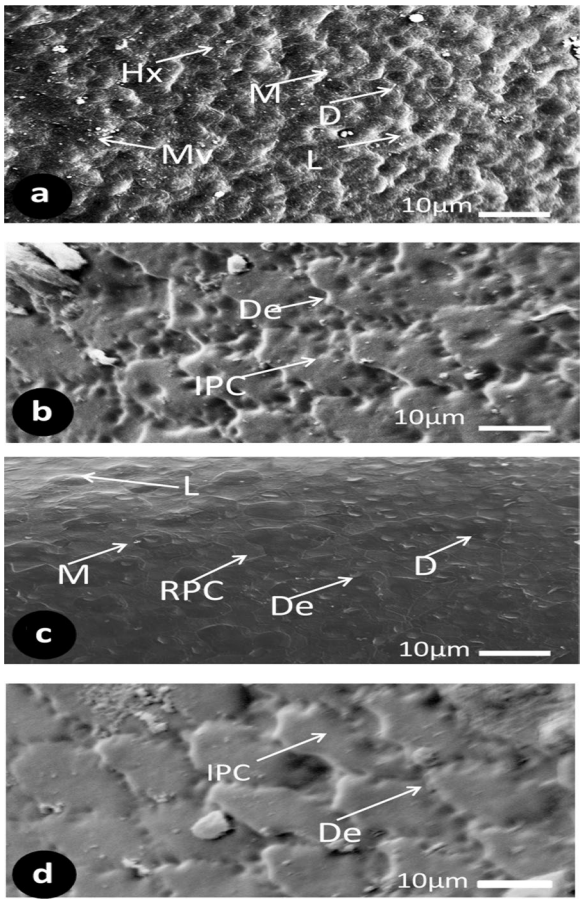


**Fig. 9** SEM micrographs of the corneal epithelial cells of four species of reptiles showing **a** *Chalcides ocellatus*; **b** *Chameleon*; **c** *Chelonia mydas*; **d** *Testudo kleinmanni*. Note: Regular polygonal epithelial cells (RPC), hexagonal epithelial cells (Hx), irregular polygonal epithelial cells (IPC), depression (De), microvilli (Mv) and three types of polymorphic cells of microplicae according to the scatter electron, (L) light type, (M) medium type and (D) dark type (Scale bar = 10 µm)

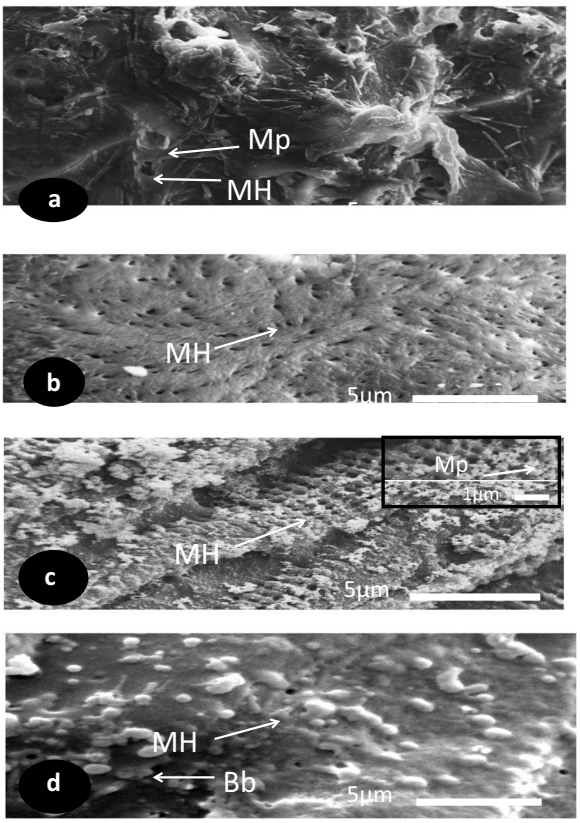


**Fig. 10** SEM micrographs of the corneal epithelial cells of four reptilian species showing **a** *Chalcides ocellatus*; **b** *Chameleon*; **c** *Chelonia mydas*; **d** *Testudo kleinmanni*. Note: Microholes (MH), micrpblicae (Mp) and Blebs (Bb). (Scale bar = 5 µm). The intercept showing higher magnification of SEM micrograph of c: *Chelonia mydas*

of polymorphic cells, according to the scatter electron on the corneal surface, which are light (L), medium (M) and dark (D) in *C. ocellatus* and *C. mydas*. The light type is distinguished by abundant microprojections covering the corneal surface, whereas the dark type is made up of dark epithelial cells with reduced density of microplicae. The semi-dark cells that make up the medium cells are covered in microplicae at a moderate density. Microvilli diffuse on the corneal surface of *C. ocellatus*, besides blebs dispersed at the corneal surface of *T. kleinmanni*, with small diameter 0.90 ± 0.05 µm (Figs. 9a, 10d, Table 4).

The examined reptilian species central corneal surfaces varied in pattern, diameter and distribution of microholes, and this variation was statistically significant ($P < 0.000$) among the different species. Moreover, microholes are surrounded by overlapping elongated microplicae (Mp) in *C. ocellatus* with a higher diameter of 4.9 ± 0.7 µm (Fig. 10a). On the other hand, the central corneal surface came out as a surface fenestrated by microholes with small diameters 0.8 ± 0.1 µm in *C. chameleon* (Fig. 10b); aligned in rows with equal diameters 1.0 ± 0.2 µm, regularly shaped and surrounded by short microplicae in *C. mydas* (Fig. 10c and its intercept); and diffused randomly with blebs of various diameters 0.3 ± 0.02 µm and shapes in *T. kleinmanni* (Table 4).

## 4 Discussion

The corneal structure of reptiles like snakes, turtles and desert monitors has only been the subject of a few published investigations [5, 12, 42–45]. Generally, the reptilian eye is very similar to that of mammals, although there are differences. The iridocorneal angle has some similarities to that of mammals, although it is less well-developed [46, 47].

According to Lawton and Martin (2006), although the Descemet's membrane is present in geckos [48] and the retina is avascular (Panagiotis), the reptile cornea

is thin and almost devoid of the Bowman's layer and Descemet's membrane of the cornea. The existence of ossicles in the sclera, which preserve the shape and size of the eye, is one of the primary anatomical differences.

The present study's objective is to determine how environmental condition affect the corneal structure of various reptilian species. The reptilian cornea anatomically resembles other vertebrates in its structure and composition, and it acts as a refracted lens for terrestrial species, not only for aquatic ones [14]. Histologically, All animals exhibit similar patterns in their corneal epithelia, stroma, and endothelial cells, despite they differ in density and thickness. Although reptile corneal layers' cellular patterns were visible throughout the experiment, certain variations in endothelial cell density, keratocyte distribution, and stroma appearance were observed. The differences in cellular densities between our results and those of previous investigations may be partially explained by variations in microhabitat, age, or animal species.

The corneas of *C. ocellatus* and *C. chameleon* were represented by the simple squamous epithelium of cuboidal cells with basal nuclei, while the corneas of *Chelonia mydas* and *Testudo kleinmanni* were illustrated by stratified squamous epithelial layer. These architecture arrangements were similarly recorded in terrestrial reptiles, e.g., *Caretta* and *Mabuya quinquetaeniata* [49]. According to El-Dawi [50], the underlying layers of the cornea are protected from the high temperatures of the environment by an increase in the quantity and variety of epithelial cells.

Concerning stromal matrix, it is arranged as parallel collagen fibrils with uniformly distributed keratocytes in the three investigated species *C. ocellatus, C. mydas* and *T. kleinmanni*. The parallelism and complexity of stromal lamellae aid in tissue stiffness and dehydration of stroma to ensure a sharp retinal image for adaptation with the diversity of environmental conditions. Many authors recoded the same arrangement and the complexity of the stromal lamellae in other reptiles as *Periophthalmus waltoni* [10, 51]. In contradiction with the present results, in *Chamaeleo calyptratus*' the keratocytes in anterior and posterior stroma were absent [5].

The present data revealed that middle stromal lamellar zones contained condensed fibrils and keratocytes, which are uniformly distributed in the stromal matrix. These results came in agreement with the findings of Akhtar, Khan [5] in case of *Chamaeleo calyptratus*. The only middle stromal lamellae that had long processes and very long cells (keratocytes) were joined to form a continuous layer in the stroma, and their keratocytes had a big nucleus and endoplasmic reticulum. There were several parallel lamellae in the middle and posterior stroma.

The epithelium, stroma and endothelium are the three layers that make up the cornea of the *C.chameleon*, according to the findings of the present study. In contrast to Akhtar and Khan's [5] findings, as observed in other animals, the available data showed that the corneal stroma of *C. chameleon* is characterized by two lamellar zones; loosed outer lamellae zone (OLZ) and compacted inner lamellae zones (ILZ). Similar to forested reptiles, *C. chameleon* has a high ability to hide from enemies. This is aided by their lamellar organization and its large interfibrillar spaces that allow the entrance of more light to form a sharp retinal image, hence improving corneal transparency [52, 53]. The cornea of the *C. chameleon's* gives the total refractive power of their eyes to compensate for other negative power of the lens. The chameleon uses this method to recognize and distinguish prey from the background without moving its head or body [5]. The stroma, inner epithelium and endothelium, which is covered with microvilli, are the three layers of the ball python's (*Python regius*) cornea, according to the available knowledge [45]. The cornea of the veiled chameleon (*Chamaeleo calyptratus*) is exceedingly thin and is made up of endothelium, Descemet's membrane, stroma and epithelium, according to Akhtar, Khan [5]. According to their data, the cornea's stroma made up 82.0% of the cornea while the epithelium made up 16.64% of it. The epithelial cells were separated by the cell and were either dark or electron-dense. These data corroborated the findings of the current investigation, which showed that the thickness of stroma varies in descending order from 94.8, 82.6 and 77.7% for *Testudo kleinmanni*, *Chalcides ocellatus* and *Chelonia mydas*, respectively, while *Chamaeleon* has the lowest stroma thickness 65.4%.

Regarding Bowman's membrane, it is considered as a modified part of the stromal layer, which is arranged as a basal strand of collagen lamellae and bound cellular epithelium layer in only two of the studied species, *C. ocellatus* and *T. kleinmanni* (high-temperature terrestrial habitat), although it is absent in *C. chameleon* (forested habitat). Similar identification was reported in the cornea of lacertilian reptiles and sea lamprey, while it was absent in geckos (forested habitat) [8, 48, 54, 55]. The Bowman's layer was also shown to be lacking in the veiled chameleon (*Chamaeleo calyptratus*), but present in humans, tree shrews, zebrafish and sharks by Akhtar and Khan [5]. Large lucent gaps found in stromal lamellae and the mucous layer of salamanderfish are similar [56]. This mucous layer keeps the cornea's upper portion moist and allows it to rotate, guarding against dryness. According to Akhtar and Khan [5], these lucent spaces could compensate for the lack of the Bowman's layer by holding mucus to prevent stromal components from drying up in hot desert or terrestrial climates. The inner layers of the eye

may also be protected by lucent spaces, which can act as a strong UV-B radiation filter (280–330 nm).

Bowman's membrane is concurrently present or absent depending on the epithelial structure and its ability to allow or impair the flow of aqueous materials to or from the stroma. These data were confirmed by Collirt and Collin [52] and Collin and Collin [8], who discuss the importance of the epithelial structure as a corneal barrier to sodium, as well as its necessity in water movement to the cellular layer. This function increases flushing of tears and corneal transparency to adapt to their higher temperature habitat. According to Kolozsvári, Nógrádi [57], many ultraviolet (UV) radiations are significantly absorbed by the epithelium and Bowman's layers in the eyes of some animals that inhabit desert climates, keeping the water in their eyes and tears from evaporating.

As discerned in the present study, a basement membrane separates the epithelium from the stroma [58]. The chameleon cornea's stroma is made up of collagen fibril lamellae. Extracellular matrix (ECM) secreted by the mesenchymal stromal cells known as keratocytes is mainly made up of proteoglycans and collagen fibrils [59]. The presence of keratocytes in the middle of the stroma suggests that they have a role in the synthesis of proteoglycans and collagen fibrils there, according to Akhtar and Khan [5].

Analyzing keratocyte density would provide useful data for numerous investigations, particularly those looking at corneal wound healing. Some comparison studies have examined the density of endothelium and superficial cells in animals using scanning electron microscopy and have addressed the influence of technical preparations for histological investigations [60–62]. The present data revealed that the stroma is packed with uniformly distributed collagen lamellae and keratocytes in both *Chelonia mydas* and *Testudo kleinmanni*. *C. ocellatus*' stromal matrix has very few keratocytes. On the other hand, *Chameleon* recorded collagen fibrils of stroma that is consists of two main zones that may be distinguished: an inner lamellar zone (ILZ) with condensed fibrils and an outer lamellar zone (OLZ) with loose fibrils. Their keratocytes are uniformly distributed in the stromal matrix. In other species, within the matrix substance, the stromal keratocyte nuclei were visible as hyperreflective structures. The density of keratocytes could be measured, and it was discovered that the anterior stroma had a higher density than the posterior stroma [62].

Descemet's membrane (DM) helps maintain the phenotype and function of corneal endothelial cells under a variety of physiological or environmental conditions [34]. DM could prevent the infiltration of certain proteins from the aqueous humor into the corneal stroma [63–65]. The distinctive corneal endothelium is anchored by DM, a particular basement membrane of the corneal endothelium, which is mostly composed of glycoproteins arranged within a three-dimensional filamentous network and collagen types III and VIII and serves as a stable scaffold during morphogenesis [66]. Corneal endothelial cells produce Descemet membrane both during prenatal and after birth [67], and it thickens with age 32 [68]. In the present study, the Descemet membrane was described as a band of collagen fibers in the two species that were examine, *C. ocellatus* (lizards) and *T. Kleinman*, where it is considerably thicker in *C. ocellatus* than other species, in comparison to that explained by Collirt and Collin [52] and Collin and Collin [8]. They reported that Descemet's membrane is formed of two parts; the anterior part is banded and the posterior ones are not banded. The DM importance manifests in the form of mechanical strength for endothelium layers and in preserving the stromal integrity and phenotype of the endothelium, which helps in controlling the eye shape during their movement in a different habitat. The current findings are consistent with and parallel to those of Lawton and Martin [47] in Saura (lizards) and rhyncocephalia (*Sphenodon punctatus*), in contrast to geckos which lack it.

It is generally known that the neural crest gives rise to corneal endothelial cells, which develop into a monolayer of hexagonal cells on the cornea's posterior surface [69]. Our findings demonstrate that the endothelial layer in the reptile cornea is composed of a single layer of flat squamous cells. Similar findings have been recorded in different vertebrate groups by Collirt and Collin [52]; Collin and Collin [8]; El-Dawi [10] and Yee, Edelhauser [41], such as amphibians, reptiles, birds, mammals, as well as fishes. They suggested that squamous cells play a vital role in the corneal transparency by controlling the hydration process and pulling bicarbonate ions and water from the stroma. Moreover, squamous cells separate the stroma from the aqueous humor to adapt to their terrestrial and aquatic habitat.

Regarding the central corneal thickness of the studied reptilian species, the findings show a high statistically significant variation, where the epithelial layer recorded the lowest thickness in *C. ocellatus* and the highest thickness in *T. kleinmanni*. In addition, the stromal thickness recorded a higher measurement in *T. kleinmanni* and a lower one in *C. ocellatus*. Moreover, the endothelium layer registered high thickness in *T. kleinmanni* and low thickness in *C. ocellatus*. Our results indicated that the examined reptilian species *T. kleinmanni* possesses high corneal thickness, for the purposes of protecting the rest of optical parts due to its higher temperature environment (arid terrestrial habitat), increasing its corneal transparency by increasing the dehydration of the

stromal layer and its refractive power and providing more lubrication for the cornea. Moreover, the present data conform to other studies [8, 52, 70] with regard to *Ctenophorus ornatus* (Terrestial habitat).

The reported high corneal thickness of *T. kleinmanni* may be due to the presence of climatic variations. In accordance with the animal's habitat, whether terrestrial, aquatic or semi-aquatic, Al-Zahaby and Elsayed [21] reported that Testudines species exhibit considerable histological changes. Whereas tortoises live on the land [18–20], turtles inhabit purely aquatic environments [71–73], and the third are semi-aquatic species [74, 75].

The histochemical structure of the examined species revealed that the epithelium has high polysaccharide content in *T. kleinmanni* (higher temperature terrestrial habitat) and moderate content in the other investigated species. As for stroma, it contains a high amount of carbohydrates in *C. mydas*, but less amount in *C. ocellatus*. All of the investigated reptile species, with the exception of the *C. chameleon*, had high endothelium layer affinities to PAS activity. Only Bowman's and Descemet's membranes, two basement membranes, are stained with PAS in *C. ocellatus*.

It is observed that polysaccharides are considered the primary energy source for different vital metabolic activities (aerobic glycolysis) in the corneal layers [15]. The polysaccharide contents might increase with increasing the metabolic activities and biochemical reactions in the cornea as in terrestrial *T. kleinmanni* [76–78]. Furthermore, the stroma represented the main bulk of cornea which is composed of collagen lamellae embedded in polysaccharides matrix, as observed in *C. mydas* [78]. These findings are compatible with previous recordings obtained by Peng, Katsnelson [15] and Lee, Wells [79]

Regarding the scanning electron microscopy investigations, the recorded variations in the cell density among investigated reptilian species are due to differences in mean cell size and shapes. These variations affect epithelial cell packing [8, 80]. In the present study, low epithelial cell density is noticed in *C. mydas* (aquatic species) and a higher cell density was found in *C. chameleon* (terrestrial species). Analysis of these results shows high statistically significant variance, which indicates the variation in osmotic stress on the corneal layers as in aquatic species (*Crocodilus porosus*) [8, 61].

Our results show an epithelial cell density of the terrestrial species that is higher than that of the aquatic ones. This variation aids in providing minimum evaporation and more corneal strength for terrestrial habitats to control the eye shape [8, 61]. Moreover, the central corneal epithelial cells have a wide range of shapes, which appear as a hexagonal in *C. ocellatus*, and as an irregular polygonal cell in *C. Chameleon* (forested habitat) and *T. kleinmanni*. The same result is found in ornated lizard *Ctenophorus oratus* (forested habitat) [8]. However, they are of regular polygonal shape in *C. mydas* (aquatic habitat), which is similarly illustrated in the cornea of the crocodile, *Crocodilus porosus* and *Acanthodactylus boskianus* [8, 11]. They proposed that the regularity and hexagonality of corneal epithelial cells aid in regulating light entrance and forming a sharp retinal image.

The observed depressions in the present study came in accordance with Pfister [81] and Akpek, Klimava [82], where they traced such cell membrane breaks to the variety of the corneal surface changes to adapt to the different environmental conditions, in only three examined reptilian species, e.g., *C. Chameleon; T. kleinmanni* (as terrestrial habitats) and *C. mydas* (aquatic habitat). Cell membrane breaks appeared with various shapes such as round and irregular and with different diameter in the investigated species. These breaks are responsible for the secretion of mucus to lubricate the corneal surface in case of terrestrial habitat and to protect the outer corneal surface from abrasion and dryness of high osmolarity of saltwater in case of aquatic habitat [8].

Concerning corneal surface microstructures, they appeared in various types on the cornea of examined species as a form of microplicae, which represented a developmental precursor to microridges and an intermediate form between microvilli and microridges. They appeared with three types, dark, medium and light, in *C. ocellatus* (forested habitat) and *C. mydas* (high-temperature habitat). These findings are in accordance with the ornate lizard, *Ctenophorus ornatus* (high-temperature habitat), and the loggerhead turtle, *C. caretta* (aquatic habitat) [8, 11]. In agreement with the present data, the cornea's inner epithelium is covered by microvilli in some reptile species, e.g., snake *Python molurus* [45] and *Chamaeleo calyptratus* [5]. Both microplicae and microvilli are essential in terrestrial habitat to increase surface area, form sharp retinal image and exit metabolic products. Additionally, in an aquatic habitat, they aid in the absorption of oxygen and provide dehydrated stroma. These results were supported in other species, e.g., *Mabuya quinquetaeniata* and *Ctenophorus ornatus* [8, 11] and a ball python [45].

A distinguishing feature of the species under study is the distribution of microholes across the corneal surface, where they were surrounded by elongated microplicae in *C. ocellatus* and short microplicae in *C. mydas*, though by blebs in *T. kleinman*. Their diameter shows a high significant relationship among the studied species. They represent external openings for secreting mucus, which aids in lubrication of the corneal surface, protects the corneal surface by forming mucous coat, and, meantime, plays a vital role in cellular exfoliation. Similar findings

are reported in *Ctenophorus ornatus* and *Caretta* by [8]. They reported that microholes are most frequently covered by microplicae or microvilli and are responsible for the secretion of mucus to lubricate the corneal surface in case of terrestrial habitat and to protect the outer corneal surface from abrasion and dryness of the high osmolarity of saltwater in the case of aquatic habitat.

In addition, Al-Zahaby, Elsayed [21], found similar microholes and microplicae that are responsible for the secretion of mucous. They proposed that massive mucous secretion lubricates organ's surface of *Testudines* living under different micro-climatic circumstances [83, 84]. However, as noted in the present study, cornea's epithelium contained small projections or microvilli in some reptilian species, e.g., lacertilians [85, 86], chelonians [87], and veiled chameleon (*Chamaeleo calyptratus*) [5]. Later authors reported that such microprojections are covered by lipid and glycocalyx that are represented by electro dense granular material. Microholes, microplicae and blebs that form on the corneal epithelial surface help to stabilize the tear film, increase cell surface area and make it easier for water and metabolic products to pass through the outer cell membrane [8, 11, 81, 88].

## 5 Conclusion

The histology, histochemical and ultrastructural levels of the cornea were significantly impacted by the diverse habitats of the examined species to adapt to various environmental circumstances. The information collected will increase our awareness of the environmental restrictions on the corneas of reptiles and advance our understanding of how this tissue evolved. In addition, to the best of our knowledge, our work is the first to assess the endothelial cell density in *Testudo kleinmanni* and *Chelonia mydas* that may aids in providing minimum evaporation and more corneal strength to control the eye shape.

**Abbreviations**

| | |
|---|---|
| EP | Epithelium |
| S | Stroma |
| DM | Descemet's membrane |
| EN | Endothelium |
| K | Keratocytes |
| Sq | Squamous cells |
| Py | Polyhedral cells |
| Bc | Basal columnar cells |
| B | Bowman's membrane |
| OLZ | Outer lamellar zone of stroma |
| ILZ | Inner lamellar zone of stroma |
| IS | Interfibrillar space |
| HX | Hexagonal cells |
| RPC | Regular polygonal cells |
| CN | Central nuclei |
| Mv | Microvilli |
| CB | Cell borders |
| MH | Microholes |
| Ci | Cilia |
| MR | Microridges |
| Bb | Blebs |

**Acknowledgements**
Not applicable.

**Author contributions**
ZA did interpretation of laboratory results and statistical analysis of data, and drafting of manuscript. AR was involved in data curation and analysis. REA and ASA participated in the design of the study, writing, reviewing. AME was involved in conceptualized, reviewing, editing, designed the methodology, and prepared the original draft of manuscript. The authors have read and approved the manuscript.

**Funding**
This research not received specific grant from any funding agency in the public, commercial or not-for-profit sectors.

**Availability of data and materials**
All data generated or analyzed during this study are included in this published article.

## Declarations

**Ethics approval and consent to participate**
All animal procedures were conducted in accordance with the standards set in the guidelines for the care and use of experimental animals by the Animal Ethics Committee of the Zoology Department in the Faculty of Science at Beni-Suef University (under an approval number is BSU/FS/2015/9.

**Consent for publication**
Not applicable.

**Competing interests**
The authors declare that they have no competing interests.

Received: 1 August 2023 Accepted: 12 March 2024
Published online: 08 May 2024

**References**

1. Duellman WE, Trueb L (1994) Biology of amphibians. JHU Press, Baltimore
2. Rosencrans RF et al (2018) Quantifying the relationship between optical anatomy and retinal physiological sensitivity: a comparative approach. J Comp Neurol 526(18):3045–3057
3. Geiger H, Koehler A, Gunzer M (2007) Stem cells, aging, niche, adhesion and Cdc42: a model for changes in cell-cell interactions and hematopoietic stem cell aging. J Cell Cycle 6(8):884–887
4. Hatami-Marbini H, Etebu E (2013) Hydration dependent biomechanical properties of the corneal stroma. Exp Eye Res 116:47–54
5. Akhtar S et al (2017) Cornea and its adaptation to environment and accommodation function in veiled chameleon (*Chamaeleo calyptratus*): ultrastructure and 3D transmission electron tomography. Microsc Res Tech 80(6):578–589
6. Beuerman RW, Pedroza L (1996) Ultrastructure of the human cornea. J Microsc Res Tech 33(4):320–335
7. Collin SP, Collin HB (1998) A comparative study of the corneal endothelium in vertebrates. J Clin Exp Optom 81(6):245–254
8. Collin SP, Collin HB (2006) The corneal epithelial surface in the eyes of vertebrates: environmental and evolutionary influences on structure and function. J Morphol 267(3):273–291
9. Saadi-Brenkia O, Hanniche N, Lounis S (2018) Microscopic anatomy of ocular globe in diurnal desert rodent *Psammomys obesus* (Cretzschmar, 1828). J Basic Appl Zool 79(1):43
10. El-Dawi E-SFA (2004) Comparative studies on the structural adaptation of the cornea of the amphibious mudskipper fish, *Periophthalmus waltoni* and the *maculated toad, Bufo regularis*. J Egypt J Aquat Biol Fish 8(2):207–235
11. El Bakry A (2014) Comparative study of the structural features of the corneal epithelium in some vertebrates. Egypt J Zool 174(1661):1–32

12. Akhtar S et al (2016) Ultrastructure features and three-dimensional transmission electron tomography of Dhub Lizard *(Uromastyx Aegyptia)* cornea and its adaptation to a desert environment. Microsc Microanal 22(4):922–932
13. Carmona FD et al (2010) Development of the cornea of true moles (Talpidae): morphogenesis and expression of PAX6 and cytokeratins. J Anat 217(5):488–500
14. Wyneken, J. Reptilian eyes and orbital structures. In Proceedings. 2012.
15. Peng H et al (2013) FIH-1/c-kit signaling: a novel contributor to corneal epithelial glycogen metabolism. J Invest Ophthalmol Vis Sci 54(4):2781–2786
16. Margaritis LH, Politof TK, Koliopoulos JX (1976) Quantitative and comparative ultrastructure of the vertebrate cornea. I. Urodele amphibia. Tissue Cell 8:591–602
17. Čejková J, Čejka Č (2015) The role of oxidative stress in corneal diseases and injuries. Histol Histopathol 30(8):893–900
18. Beisser JC, Lemell P, Weisgram J (2004) The dorsal lingual epithelium of *Rhinoclemmys pulcherrima* incisa (Chelonia, Cryptodira). Anatom Rec Part A Discov Mol Cell Evol Biol 277(1):227–235
19. Bels VL, Davenport J, Delheusy V (1997) Kinematic analysis of the feeding behavior in the box turtle *Terrapene carolina* (L.), (Reptilia: Emydidae). J Exp Zool 277(3):198–212
20. Sabry DA et al (2015) Comparative studies of tongue of *Gopherus gopherus* (turtle), Mus musculus (mice), *Erinaceus auritus* (hedgehog) *and Psammomys obesus*. J Biosci Appl Res 1:160–167
21. Al-Zahaby SA, Elsayed NS, Hassan SS (2018) Morphological, histological and ultrastructural (SEM) characterization of the Egyptian tortoise's tongue. Int J Zool Stud 3(2):101–111
22. Repérant JP, et al. comparative analysis of the primary visual system of reptiles. In: Biology of the reptilian. Biology of the reptilia: neurology C: sensorimotor integration, vol. 17. Chicago: University of Chicago Press; 1992.
23. El Din SB (2006) A guide to the reptiles and amphibians of egypt. Oxford University Press, Oxford
24. Leviton AE, et al. Handbook to middle east amphibians and reptiles. St. Louis Society for the Study of Amphibians and Reptiles. 1992.
25. Hillenius D, Gasperetti J (1984) Reptiles of Saudi Arabia: the chameleons of Saudi Arabia. J Fauna Saudi Arabia 6:513–527
26. Ballen CJ et al (2016) Multifactorial sex determination in chameleons. Journal Herpetol 50(4):548–551
27. Swash A, Still R (2005) Birds, mammals, and reptiles of the Galápagos Islands: an identification guide. Yale University Press, New Haven
28. Uwe F, Havas P (2007) Checklist of Chelonians of the world. J Vertebr Zool 57(2):149–368
29. Baha-El-Din S, Attum O, El-Din MB (2003) Status of *Testudo kleinmanni* and *T. werneri* in Egypt. J Chelonian Conserv Biol 4(3):648–655
30. Perälä J (2005) Assessment of the threatened status of *Testudo kleinmanni Lortet, 1883 (Testudines: Testudinidae) for the IUCN Red List*. J Chelonian Conserv Biol 4:891–898
31. Perälä J (2001) A new species of Testudo (*Testudines: Testudinidae*) from the Middle East, with implications for conservation. J Herpetol 15:567–582
32. van der Kuyl AC et al (2002) Phylogenetic relationships among the species of the genus Testudo *(Testudines: Testudinidae)* inferred from mitochondrial 12S rRNA gene sequences. J Mol Phylogenet Evol 22(2):174–183
33. Suvarna S, Layton C. Bancroft's theory and practice of histological techniques. In: Aughey E, Frye FL, editors Comparative veterinary histology, vol 21. Churchill Livingstone. J Elsevier. Manson Publishing. 2013. p. 173–186.
34. Passo RM, et al. Electron beam irradiated corneal versus gamma-irradiated scleral patch graft erosion rates in glaucoma drainage device surgery. 2019. p. 1–6.
35. Bancroft JD, Layton C (2013) The hematoxylin and eosin. In: Suvarna SK, Layton C, Bancroft JD (eds) Theory & practice of histological techniques, 7th edn. Churchill Livingstone of El Sevier, Philadelphia, pp 172–214. https://doi.org/10.1016/B978-0-7020-4226-3.00010-X
36. McManus J (1946) Histological demonstration of mucin after periodic acid. J Nat 158(4006):202
37. Morris JK (1965) A formaldehyde glutaraldehyde fixative of high osmolality for use in electron microscopy. J Cell Biol 27:1A-149A
38. Jeffree CE, Read ND (1991) Ambient-and low-temperature scanning electron microscopy. J Electron Microsc Plant Cells 313:413
39. Goldstein JI et al (2017) Scanning electron microscopy and X-ray microanalysis. Springer, New York
40. Abràmoff MD, Magalhães PJ, Ram S (2004) Image processing with ImageJ. J Biophoton Int 11(7):36–42
41. Yee RW, Edelhauser HF, Stern ME (1987) Specular microscopy of vertebrate corneal endothelium: a comparative study. Exp Eye Res 44(5):703–714
42. Pcheliakov V (1979) Characteristics of the structure of the cornea of the reptilian eye. Arkhiv Anatom Gistol Embriol 76(5):86–91
43. Foureaux G et al (2010) Rudimentary eyes of squamate fossorial reptiles *(Amphisbaenia and Serpentes)*. Anatom Rec Adv Integr Anat Evol Biol 293(2):351–357
44. El-Bakry AM (2011) Comparative study of the corneal epithelium in some reptiles inhabiting different environments. Acta Zool 92(1):54–61
45. Da Silva MAO et al (2014) The spectacle of the ball python *(Python regius):* a morphological description. J Morphol 275(5):489–496
46. Millichamp N, Jacobson E. Ophthalmic diseases of reptiles. J Kirk RW. Current Veterinary Therapy IX. Small Animal Practice. Saunders. Philadelphia, 1986: p. 621–624.
47. Lawton A, Martin P (2006) Reptilian ophthalmology. J Reptile Med Surg 20:323–342. https://doi.org/10.1016/B0-72-169327-X/50024-9
48. Duke-Elder S. System of ophthalmology: Vol. 1: the eye in evolution, and Vol. IV: physiology of the eye and of vision. J Henry Kimpton. London; 1958. p. 605–706.
49. El Bakry A (2011) Comparative study of the corneal epithelium in some reptiles inhabiting different environments. Acta Zool J 92(1):54–61
50. El-Dawi E-SFA (2005) Comparative studies on the corneal structural adaptation of two rodents inhabiting different environments. J Egypt J Hosp Med 20:131–147
51. Koudouna E et al (2018) Evolution of the vertebrate corneal stroma. J Progress Retin Eye Res 64:65–76
52. Collirt SP, Collin H (2001) The fish cornea: adaptations for different aquatic environments. J Sens Biol Jawed Fish New Insights 57–97
53. Meek KM, Knupp C (2015) Corneal structure and transparency. Prog Retin Eye Res 49:1–16
54. Ronning O, Hoyte DAN, Dixon AD (2017) Fundamentals of craniofacial growth. CRC Press, pp 225–256
55. Shand J (1988) Corneal iridescence in fishes: light-induced colour changes in relation to structure. J Fish Biol 32(4):625–632
56. Collin HB, Collin SP (1996) The fine structure of the cornea of the salamanderfish, *Lepidogalaxias salamandroides (Lepidogalaxiidae, Teleostei)*. Cornea 15(4):414–426
57. Kolozsvári L et al (2002) UV absorbance of the human cornea in the 240- to 400-nm range. Invest Ophthalmol Vis Sci 43(7):2165–2168
58. Soules KA, Link BA (2005) Morphogenesis of the anterior segment in the zebrafish eye. BMC Dev Biol 5(1):12
59. Massoudi D, Malecaze F, Galiacy SD (2016) Collagens and proteoglycans of the cornea: importance in transparency and visual disorders. Cell Tissue Res 363(2):337–349
60. Doughty MJ (1994) The cornea and corneal endothelium in the aged rabbit. Optom Vis Sci 71(12):809–818
61. Collin SP, Collin HB (2000) A comparative SEM study of the vertebrate corneal epithelium. J Cornea 19(2):218–230
62. Labbé A et al (2006) Comparative anatomy of laboratory animal corneas with a new-generation high-resolution in vivo confocal microscope. Curr Eye Res 31(6):501–509
63. Chen J et al (2017) Descemet's membrane supports corneal endothelial cell regeneration in rabbits. J Sci Rep 7(1):6983
64. Danielsen CC (2004) Tensile mechanical and creep properties of Descemet's membrane and lens capsule. J Exp Eye Res 79(3):343–350
65. Sawada H, Konomi H, Hirosawa K (1990) Characterization of the collagen in the hexagonal lattice of Descemet's membrane: its relation to type VIII collagen. J Cell Biol 110(1):219–227
66. Wulle K, Lerche W (1969) Electron microscopic observations of the early development of the human corneal endothelium and Descemet's membrane. J Ophthalmol 157(6):451–461
67. Wulle KG (1972) Electron microscopy of the fetal development of the corneal endothelium and Descemet's membrane of the human eye. J Invest Ophthalmol Vis Sci 11(11):897–904

68. Murphy C, Alvarado J, Juster R (1984) Prenatal and postnatal growth of the human Descemet's membrane. J Invest Ophthalmol Vis Sci 25(12):1402–1415
69. Bahn CF et al (1984) Classification of corneal endothelial disorders based on neural crest origin. J Ophthalmol 91(6):558–563
70. Kanungo J, Swamynathan SK, Piatigorsky J (2004) Abundant corneal gelsolin in Zebrafish and the 'four-eyed'fish, *Anableps anableps*: possible analogy with multifunctional lens crystallins. J Exp Eye Res 79(6):949–956
71. Weisgram J (1985) Feeding mechanics of *Claudius angustatus* Cope 1865. Fortschr Zool 30:257–260
72. Iwasaki SI, Asami T, Wanichanon C (1996) Fine structure of the dorsal lingual epithelium of the juvenile Hawksbill turtle, *Eretmochelys imbricata* bissa. Anatom Rec 244(4):437–443
73. Beisser C, Weisgram J (2001) Dorsal tongue morphology and lingual glands in Chelonians. J Morphol 248:205
74. Iwasaki SI (1992) Fine structure of the dorsal epithelium of the tongue of the freshwater turtle, *Geoclemys reevesii* (Chelonia, Emydinae). J Morphol 211(2):125–135
75. Beisser C, Lemell P, Weisgram J (2001) Light and transmission electron microscopy of the dorsal lingual epithelium of *Pelusios castaneus* (Pleurodira, Chelidae) with special respect to its feeding mechanics. Tissue Cell 33(1):63–71
76. Von Zaluskowski PRA. Glycogen metabolism in *Corynebacterium glutamicum*: effects of environmental factors and of metabolic disturbances. 2015, Universität Ulm.
77. Kinoshita JH (1962) Some aspects of the carbohydrate metabolism of the cornea. J Progress Retinal Eye Res 1(2):178–186
78. Remen M et al (2015) Effect of temperature on the metabolism, behaviour and oxygen requirements of *Sparus aurata*. J Aquacult Environ Interact 7(2):115–123
79. Lee WG et al (2019) Prevalence of diabetes in liver cirrhosis: a systematic review and meta-analysis. J Diabetes Metabol Res Rev 15:e3157
80. Simmich J, Temple SE, Collin SP (2012) A fish eye out of water: epithelial surface projections on aerial and aquatic corneas of the 'four-eyed fish'*Anableps anableps*. J Clin Exp Optom 95(2):140–145
81. Pfister RR (1973) The normal surface of corneal epithelium: a scanning electron microscopic study. J Invest Ophthalmol 12(9):654–668
82. Akpek EK et al (2009) Evaluation of patients with dry eye for presence of underlying Sjögren's syndrome. Cornea 28(5):493
83. Winokur RM (1988) The buccopharyngeal mucosa of the turtles (Testudines). J Morphol 196(1):33–52
84. Schwenk K (2000) Feeding: form, function and evolution in tetrapod vertebrates. Elsevier, New York
85. Ebbesson SO, Karten HJ (1981) Terminal distribution of retinal fibers in the tegu lizard *(Tupinambis nigropunctatus)*. Cell Tissue Res 215(3):591–606
86. Bennis M et al (1994) An experimental re-evaluation of the primary visual system of the European chameleon, *Chamaeleo chameleon*. Brain Behav Evol 43(3):173–188
87. Hergueta S et al (1995) Interspecific variation in the chelonian primary visual system. J Hirnforsch 36(2):171–193
88. Pfister R, Burstein N (1977) The normal and abnormal human corneal epithelial surface: a scanning electron microscope study. Invest Ophthalmol Vis Sci 16(7):614–622


## Publisher's Note